The Role of IL-23/IL-17 Axis in Lupus Nephritis[1]

Zheng Zhang[2], **Vasileios C. Kyttaris**[2], and **George C. Tsokos**[3]
Division of Rheumatology, Beth Israel Deaconess Medical Center and Harvard Medical School, Boston, MA 02215

Abstract

T cells that express IL-17 infiltrate the kidneys of patients with systemic lupus erythematosus. A significant proportion of these cells are $CD3^+CD4^-CD8^-$ double-negative T cells. In this study, we show that double-negative T cells from MRL/*lpr* mice express high amounts of IL-17 and that as disease progressively worsens, the expression of IL-17 and of IL-23 receptor in lymphocytes from these mice increases. Lymph node cells from lupus-prone mice, but not control mice, treated in vitro with IL-23 induce nephritis when transferred to non-autoimmune, lymphocyte-deficient $Rag-1^{-/-}$ mice. Kidney specimens from these recipient mice show significant Ig and complement deposition. The data indicate that an aberrantly active IL-23/IL-17 axis contributes to the development of nephritis in lupus-prone mice.

Lupus nephritis affects more than 50% of patients with systemic lupus erythematosus (SLE) [4] and is a major cause of morbidity (1). Despite significant advances in our understanding of the interaction of immune cells, soluble factors, and resident kidney cells, the precise pathophysiologic mechanisms that underlie the development of lupus nephritis is still unclear (2). This prevents the use of specific treatment modalities and to date treatment of lupus nephritis depends on the use of nonselective and toxic immunosuppressive regimens (3). The pathologic picture of lupus nephritis is complex with mesangial matrix expansion, mononuclear cells infiltration the tubular-interstitial area, mesangial cells proliferation in the glomeruli, and immune complexes/complement fragments depositing in the mesangial subepithelial and subendothelial space (4). No single-cell population or cytokine has been decisively identified as a key mediator in the pathophysiologic cascade in lupus nephritis.

We recently reported (5) that IL-17, a proinflammatory cytokine produced by a subtype of T cells, may play a role in the pathogenesis of lupus nephritis. Specifically, we demonstrated that T cells lacking both CD4 and CD8 from the surface membrane (double-negative T cells, DNT) from patients with SLE produce significant amounts of IL-17 and IFN-γ and expanded when stimulated in vitro with an anti-CD3 Ab in the presence of accessory cells. More importantly, IL-17 and DNT cells were found in kidney biopsies of patients with active lupus nephritis (5). These data add to previous studies which had shown that DNT cells provide help to B cells (6–8) and contribute to the abnormal autoantibody profile of lupus patients. Furthermore, it has been shown that serum of patients with SLE contains high levels not only of IL-17 and but

3Address correspondence and reprint requests to Dr. George C. Tsokos, Beth Israel Deaconess Medical Center, Division of Rheumatology, 330 Brookline Avenue, CLS-937, Boston, MA 02215. gtsokos@bidmc.harvard.edu.
2Z.Z. and V.C.K. contributed equally to this work.

Disclosures
The authors have no financial conflict of interest.

[4]Abbreviations used in this paper: SLE, systemic lupus erythematosus; DNT, double-negative T cell; PAS, periodic acid-Schiff; DAPI, 4′,6-diamidino-2-phenylindole.

also of IL-23 (9,10), a cytokine important for the development, expansion, and proliferation of Th17 cells (11). Taken together, these findings suggest that an abnormally activated IL- 23/ IL-17 axis may be contributing to the pathogenesis of lupus nephritis.

To further elucidate the role of IL-17 and in particular the role of $CD3^+CD4^-CD8^-IL-17^+$ cells in lupus nephritis, we used the well-established murine lupus model MRL/*lpr*. These mice are characterized by the introduction of a mutation in the CD95 (Fas) locus leading to defective lymphocyte apoptosis and acceleration of the underlying autoimmune phenotype (12). More than 50% of the lymphocytes that expand in the secondary lymphoid organs of these animals express neither CD4 nor CD8 on their surface (13). These DNT cells show defective production of IL-2 and IFN-γ upon stimulation. Although forming the bulk of the immune cell pool in MRL/*lpr* mice, the role of DNT in initiating and propagating the autoimmune disease is still unclear.

We hypothesized that the expanded double-negative population in MRL/*lpr* mice produces increased amounts of IL-17, infiltrates the kidneys, and contributes to nephritis. Indeed, we show that MRL/*lpr*-derived lymphocytes express IL-17, infiltrate the kidneys, and, when conditioned in vitro with IL-23, cause nephritis in a nonautoimmune mouse model.

Materials and Methods

Animals

C56BL/6J (B6), B6.MRL/*lpr*, MRL/*lpr*/2J (MRL), MRL/MpJ (MPJ), and Rag-1 knockout mice were purchased from The Jackson Laboratory and housed in the specific animal facility of Beth Israel Deaconess Medical Center. All animal procedures used in the study were approved by the Institutional Animal Care and Use Committee at Beth Israel Deaconess Medical Hospital.

Urine analysis

Urine that was collected from each group of mice was analyzed for protein, blood, and cell concentrations using the Multistix 10 SG reagent strips and the Clinitek Status analyzer (Bayer Healthcare). Proteinuria was expressed as: 0, none; +, 30–100 mg/dl; ++, 100–300 mg/dl; +++, 300–2000 mg/dl; and ++++, >2000 mg/dl.

Morphology and immunohistochemistry

Longitudinal sections of the kidneys, cut through the papilla, were fixed in 4% buffered paraformaldehyde and then embedded in paraffin. The kidney sections were subsequently cut at 3-µm thickness. The kidney sections were stained with H&E and periodic acid-Schiff (PAS). The number of mesangial cells in the glomeruli was determined by counting their nuclei within the glomerulus. The Nikon NIS-Elements Basic Research program was used to evaluate the area of glomeruli. One hundred glomeruli were evaluated in each group.

For immunofluorescent staining, kidney samples were snap frozen at −70°C before being cut at 6 µm with a cryostat and fixed in acetone. Samples were blocked with 10% FBS in PBS for 30 min, then incubated with prelabeled anti-CD3 FITC Ab and nonlabeled primary Ab against IL-17 (JC11-18H10.1; BD Biosciences) at a 1/100 dilution overnight at 4°C. After washing with PBS, secondary Ab (Texas Red-labeled goat anti rat IgG was purchased from Jackson Immunoresearch Laboratories) was added at a 1/100 dilution for 1 h. For IgG, IgM, and C3d staining, prelabeled Abs were used. Afterward, the sections were stained with 4′,6-diamidino-2-phenylindole (DAPI, 0.5 µg/ml; Invitrogen) and mounted on a slide with anti-fade solution (Slowfade Gold; Invitrogen). Finally, the slides were scanned using an Nikon Eclipse Ti confocal microscope and the images were analyzed with EZ-C1 version 3.6

software. The prelabeled anti-mouse IgG Alexa Fluor 488 and anti-mouse IgM Alexa Fluor 488 Abs were purchased from Invitrogen. Anti-mouse C3d Ab was purchased from MP Biomedicals.

Cell extraction from tissues

Cells were extracted from murine spleens and lymph nodes by filtering the tissue through a 100-µm BD Biosciences Falcon cell strainer. The extracts were centrifuged at 1200 rpm for 5 min. ACK lysing buffer (Quality Biological) solution was added in the cell pellet to lyse the RBC. The treated cell pellet was subsequently washed once with DMEM cell culture medium and resuspended in DMEM cell culture medium for further treatment or staining.

Murine kidney tissue was incubated with collagenase type IA (10 µg/ ml; Sigma-Aldrich) in cold Dulbecco's PBS buffer with EDTA (2 µM) for 15 min at 37°C. The digested kidney tissue suspension was teased through a 100-µm BD Biosciences Falcon cell strainer (Fisher Scientific) using the rubber end of a 1-ml syringe plunger. The cells were centrifuged at 1200 rpm for 5 min. The cell pellet was washed with 2% FCS in PBS. Fresh kidney suspensions were stained with anti-CD3, anti-CD4, anti-CD8 (surface staining), and IL-17 Abs (intracellular cytokine staining, see relevant section of *Materials and Methods*), then analyzed by FACS.

Cell culture

Murine lymphocytes, when mentioned, were cultured in DMEM with 10% (v/v) FCS supplemented with 50 µM 2-ME, 1 mM sodium pyruvate, non-essential amino acids, L-glutamine, 100 U per ml of penicillin, and 100 µg of streptomycin per ml at 37°C in a humidified atmosphere of 10% CO_2 in culture incubator.

IL-23 expansion and measurement of cytokine production

Cells extracted from lymph nodes were plated at the concentration between 2×10^6 and 4×10^6 cells/ml. Anti-CD3 was added in the solution at a concentration of 2 µg/ml. IL-23 (20 ng/ ml; R&D Systems) was also added in the solution at days 0, 2, and 4. At day 5 or 6, cells were suspended at a concentration of 2×10^6/ml and stimulated with PMA/calcium ionophore A23187 and 1 µl/ml brefeldin A (Golgi-Plug; BD Pharmingen) for 4 h. The cells were subsequently collected and IL-17 production was measured by intracellular cytokine staining.

Immunofluorescent staining, flow cytometry analysis, and cell proliferation assay

Cell surface marker and intracellular staining for murine lymphocytes isolated from the spleen and the lymph nodes were done with anti-mouse CD3, CD28, CD4, CD8, and IL-17 Abs (BD Pharmingen). Flow cytometric experiments were performed using an LSRII flow cytometer (BD Biosciences) and FlowJo version 7.2.2 (Tree Star).

For cell proliferation assays, we used CFSE staining. In brief, lymphocytes were suspended at a concentration of 5×10^7/ml in PBS. CFSE (Molecular Probes) was added at a final concentration of 5 µM and incubated at 37°C for 5 min. At the end of the incubation period, the cells were washed three times in cold complete DMEM. Cells were incubated at a concentration of 2×10^6/ml in the presence/absence of anti-CD3, anti-CD28, and IL-23.

Intracellular cytokine staining

For intracellular cytokine staining, cells were isolated from lymph nodes and spleen, then were stimulated for 4 h at 37°C, in a humidified atmosphere of 10% CO_2, in culture medium containing PMA (50 ng/ml; Sigma-Aldrich), ionomycin (1 µg/ml; Sigma-Aldrich), and brefeldin A (Golgi- Plug, 1 µl/ml; BD Pharmingen). After staining of surface markers (CD4,

CD3, CD8), the cells were fixed and made permeable with Cytofix/Cytoperm and Perm/Wash buffer according to the manufacturer's instructions (BD Biosciences). Anti-IL-17 (JC11-18H10.1) Ab was added in the solution at a dilution of 1/200. The permeabilized cells were incubated for 20 min at 4°C and were washed twice in Perm/Wash before analysis.

Quantitative real-time PCR

Total mRNA was extracted using a RNeasy Mini Kit (Qiagen). Reverse transcription was performed using a TaqMan Reverse Transcription Kit (Applied Biosystems) in a total reaction volume of 100 µl with 2 µg of total RNA. Quantitative real-time PCR was performed in a total reaction volume of 25 µl using TaqMan fast mix (Applied Biosystems). The Applied Biosystems 7500 Fast system was used for TaqMan analysis. Gene expression was normalized to expression of the gene *Actb* (encoding mouse β-actin; Applied Biosystems). The specific primers used were as follows: IL23R, forward 5′-TCCGA GGAGTCAGTGCTAAA-3′ and reverse, 5′-AGAACGTCTTCCAGGGTGAA-3′; probe, 5′-FAM – TGAGCACCTGCTTCATCAGGTAGCATAMRA- 3′; IL-17A, forward, 5′-CTCCAGAAGGCCCTCAGACTAC-3′ and reverse, 5′-AGCTTTCCCTCCGCATTGACACAG-3′; and probe, 5′-FAM-TCTGGGAAGCTCAGTGCCGCCACCAGC-TAMRA-3′.

Adoptive transfer

Lymph node cells were extracted and cultured with soluble anti-CD3 (2 µg/ml). In addition, IL-23 (20 ng/ml in DMEM) or complete DMEM was added at day 0. After 48 h, the cells were washed with PBS twice and were counted. Subsequently, 5 million cells were suspended in 200 µl of PBS, and transferred into each Rag-1$^{-/-}$ mouse by i.p. injection.

Statistical analysis

The results are expressed as mean ± SD in the text and figures. ANOVA used to evaluate differences. Statistical correlations were assessed using the Pearson product-moment correlation coefficient.

Results

IL-17 expression is increased in lupus-prone mouse-derived T cells

To address whether Th17 cells are involved in the pathogenesis of SLE and in particular lupus nephritis, we used MRL/*lpr* and B6/*lpr* mice which develop readily lupus-like features. Both murine strains are characterized by the expansion of a population of T cells that do not express the CD4 and CD8 markers on their surface. Interestingly, these so-called DNT have been found to express IL-17 in the kidneys of patients with lupus nephritis (5).

First, we measured the expression of IL-17 as a signature cytokine of Th17 lineage in lupus-prone MRL/*lpr* animals. We isolated cells from both lymph nodes and spleens of eight control (MRL/MPJ) and nine lupus-prone mice (all animals were 4 mo old).

We then briefly stimulated the lymphocytes in vitro with PMA and calcium ionophore and analyzed the IL-17 expression using intracellular staining. In Fig. 1, *A* and *B*, we show that lymphocytes derived from the lymph nodes of MRL/*lpr* mice expressed IL-17 at significantly higher levels than control lymphocytes from MRL/MPJ lymph nodes. This was true for both CD4$^+$ T cells (percentage of MRL/*lpr*-derived T cells expressing IL-17A vs MRL/MPJ-derived T cells expressing IL-17A: 0.33 ± 0.05 vs 0.19 ± 0.018, *p* < 0.01) and DNT cells (percentage of MRL/*lpr*-derived T cells expressing IL-17A vs MRL/MPJ-derived T cells expressing IL-17A: 1.25 ± 0.11 vs 0.4 ± 0.05, *p* < 0.001).

Similarly, splenocytes expressing IL-17A were significantly more in MRL/*lpr* vs MRL/MPJ (Fig. 1, *C* and *D*) mice. Again, both CD4^{+} (percentage of MRL/*lpr* derived T cells expressing IL-17A vs MRL/MPJ derived T cells expressing IL-17A: 0.65 ± 0.05 vs 0.18 ± 0.014, $p < 0.01$) and DNT cells (percentage of MRL/*lpr*-derived T cells expressing IL-17A vs MRL/MPJ-derived T cells expressing IL-17A: 2.2 ± 0.18 vs 0.87 ± 0.1, $p < 0.005$) showed similar differences between lupus-prone and control mice. Upon assessing the relative expression of IL-17A between the two cell subtypes, it was apparent that the DNT cells expressed significantly more IL-17A than CD4^{+} T cells in both lupus-prone and control mice ($p < 0.001$ for all groups).

Contrary to IL-17A production, the DNT cells from both lymph nodes and spleens of MRL/*lpr* and MRL/MPJ mice did not produce significant amounts of IL-2 upon stimulation for 48 h with anti-CD3 and anti-CD28 Abs (IL-2 secretion by MRL/*lpr*-derived DNT cells vs MRL/*lpr*-derived CD4^{+} T cells: 10.66 ± 2.54 pg/ml vs 4373.85 ± 456.02 pg/ml, $p = 0.0003$). Similarly, IFN-γ was secreted at very low levels by DNT cells (IFN-γ secretion by MRL/*lpr*-derived DNT cells vs MRL/*lpr*-derived CD4^{+} T cells: 7.20 ± 1.33 pg/ml vs 2620.96 ± 312.7 pg/ml, $p < 0.0005$).

Given that lupus-prone mice differ from control mice in that the majority of T cells are DNT, we compared the two groups with regard to total number of cells expressing IL-17A. We extracted and counted the cells from both lymph nodes and spleens of nine MRL/*lpr* mice and eight control MPJ mice. As expected, we found that CD3^{+}CD4^{−}CD8^{−} population was expanded in MRL/*lpr* mice (24–58% of CD3^{+} population, nine mice, 4-mo-old MRL/*lpr* mice) as opposed to control mice (1.4–6% of CD3^{+} population, eight mice, 4-mo-old MRL/MPJ mice). We then analyzed the expression of IL-17A in CD4^{+} and CD3^{+}CD4^{−}CD8^{−} cells as above. In Fig. 1*E*, we show that the overall number of MRL/*lpr* lymphocytes expressing IL-17A was significantly higher than the number of MRL/MPJ IL-17A^{+} lymphocytes (lymph node-derived IL-17A^{+} lymphocytes: MRL/*lpr* vs MRL/MPJ: $4{,}377{,}547 \pm 90{,}326$ vs $21{,}805 \pm 2{,}883$; IL-17A^{+} splenocytes: MRL/*lpr* vs MRL/MPJ: $556{,}401 \pm 9{,}692$ vs $19{,}020 \pm 2{,}555$). In addition, although both CD4^{+} and DNT cells expressed IL-17A in MRL/ MPJ mice (CD3^{+}CD4^{−}CD8^{−} IL-17A^{+} vs CD4^{+}IL-17A^{+} cells: $1{,}995 \pm 406$ vs $19{,}811 \pm 2{,}484$ in lymph nodes; $5{,}285 \pm 855$ vs $13{,}735 \pm 2{,}552$ in spleen; data from eight 4-mo-old MRL/MPJ animals), the MRL/*lpr*-derived lymphocytes had a dominant population of CD3^{+} CD4^{−} CD8^{−} IL-17A^{+} cells (CD3^{+} CD4^{−} CD8^{−} IL-17A^{+} vs CD4^{+} IL-17A^{+} cells: $3{,}730{,}215 \pm 4206$ vs $647{,}333 \pm 889$ in lymph nodes; $493{,}095 \pm 9{,}064$ vs $63{,}306 \pm 945$ in spleen; data from nine 4-mo-old MRL/*lpr* animals).

In addition to MRL/*lpr*, we evaluated the expression of IL-17A in T cells derived from both spleen and lymph nodes of another strain of lupus-prone mice, the B6/*lpr* mice. We found that B6/*lpr* lymph node-derived T cells had significantly higher expression of IL-17A when compared with control B6 mouse-derived T cells (percentage of B6/ *lpr*-derived CD4^{+} T cells expressing IL-17A vs B6-derived CD4^{+} T cells expressing IL-17A: 0.16 ± 0.03 vs 0.11 ± 0.01, $p < 0.0002$; percentage of B6/*lpr*-derived DNT cells expressing IL-17A vs B6-derived DNT cells expressing IL-17A: 0.38 ± 0.08 vs 0.32 ± 0.06, $p < 0.035$). Given the low number of DNT cells in the spleens of B6 mice, we could not measure with certainty differences between B6 DNT and B6*lpr* (data not shown).

In summary, IL-17A-expressing T cells are significantly increased in numbers in lupus-prone mice compared with control mice. Importantly, our results point to the fact that the major IL-17A-expressing population among T cells in the lymphoid organs of lupus-prone MRL/*lpr* and B6/*lpr* mice is the CD3^{+}CD4^{−}CD8^{−} cell population.

IL-17 and IL-23 receptor expression are up-regulated in lupus-prone mouse-derived T cells

Th17 cell population maintenance and expansion relies heavily on IL-23. IL-23 binds to its receptor on the surface of T cells and leads to expression of IL-17. Because we found a higher frequency of Th17 cells in lupus-prone mice compared with control mice, we evaluated whether IL-23 is involved in the up-regulation of IL-17A in murine lupus. First, we evaluated whether the IL-23 receptor is expressed in lupus-prone mouse- derived T cells and whether its expression changes as the disease progresses. Indeed, we found that lupus-prone B6/*lpr*-derived lymph node cells express IL-23 receptor mRNA; this expression increased as the mouse aged and disease became more severe (Fig. 2*A*, □). On the contrary, B6-derived lymph node cells express IL-23 receptor mRNA at almost undetectable levels. In addition, we found that IL-17A mRNA levels were also increased in B6/*lpr* mice as opposed to B6 (Fig. 2*B*, □) and that the levels increased as the mice aged. Importantly, IL-23 receptor mRNA levels in these B6/*lpr* mice of different ages correlated with the IL-17A mRNA levels from the same animals (Pearson's $r = 0.9616$, $p = 0.0384$, $n = 4$ animals/group). Contrary to this finding, IL-17F mRNA levels were not different between lupus-prone and control mice (data not shown). Second, given that the IL-23 receptor was robustly expressed at the mRNA level in lupus-prone mice, we evaluated whether treatment of cells with IL-23 would result in a further increase of IL-17A and/or expression of the IL-23 receptor. Indeed, we found that treating cells with IL-23 led to a manifold increase in the expression of IL-17A and the IL-23 receptor (Fig. 2). Again, IL-23 receptor mRNA showed a trend toward a statistically significant correlation with IL-17A mRNA levels (Pearson's $r = 0.9322$; $p = 0.0678$).

Given that the DNT population was disproportionably enriched with Th17 cells, we further evaluated whether IL-23 treatment influences CD4$^+$ and DNT cells differently. To this end, we cultured lymph node-derived cells with anti-CD3 Ab in the presence or absence of IL-23 for 6 days and measured the expression of IL-17A. Fig. 3 shows that T cells from either MRL/*lpr* or B6/*lpr* mice after incubation with IL-23 express higher levels of IL-17A in both DNT (percentage of IL-17A$^+$ B6/*lpr*-derived T cells vs control B6: 45.2 ± 1.69 vs 18.9 ± 1.1, $p < 0.0001$; MRL/*lpr* vs control MRL/MPJ: 19.1 ± 0.52 vs 15.7 ± 0.74, $p < 0.0001$) and CD4$^+$ populations than their respective controls (percentage of IL-17A$^+$ B6/*lpr*-derived T cells vs control B6: 18.2 ± 1.3 vs 3.13 ± 0.04 $n = 8$, 5 mo old, $p < 0.0001$; MRL/*lpr* vs control MRL/MPJ: 10.7 ± 1.0 vs 6.8 ± 0.7, $n = 7$, 4 mo old, $p < 0.0001$). Furthermore, we show that DNT cells express significantly higher IL-17A than CD4$^+$ cells after incubation with IL-23.

Because IL-23 treatment led to increased Th17 expression among DNT in particular but also CD4$^+$ cells, we asked whether IL-23 promotes T cell proliferation. T cells from MRL/*lpr* and control mice incubated with anti-CD3 Ab and IL-23 were cultured for 6 days. At the end of the incubation period, the cells were stained for CD4, CD3, and CD8. In Fig. 4*A*, we show that the proportion of CD3$^+$CD4$^-$CD8$^-$ cells among T cells increased significantly (from 25 to 32.8% for MRL/MPJ mice; from 54 to 72.4% for MRL/*lpr*). Thereafter, we sorted CD3$^+$CD4$^+$ and CD3$^+$CD4$^-$CD8$^-$ cells and measured their proliferation. Two hundred thousand cells were incubated in 96-well plates precoated with anti-CD3 and anti-CD28 Abs in the absence or presence of IL-23 for 6 days. We found that DNT cells expanded significantly more in the presence of IL-23 (MRL/*lpr* DNT cells cultured with IL-23 vs MRL/*lpr* DNT cells cultured without IL-23: $600,000 \pm 11,857$ cells/well vs $320,000 \pm 6,080$ cells/well, $p < 0.001$; Fig. 4*B*). In contrast, IL-23 had no effect on CD4$^+$ cells. From this set of experiments, we conclude that lupus-prone mouse T cells express high levels of IL-23 receptor mRNA and IL-17A mRNA and protein; incubation of the cells with IL-23 leads to a further significant increase in both IL-23 receptor and IL-17A expression. Finally, IL-23 acts as a trophic cytokine for DNT cells, increasing both their percentage among the total T cell population and their absolute number.

IL-17-expressing cells are present in the kidneys of lupus-prone mice with nephritis

One of the most important manifestations of SLE is nephritis. A recent publication linked nephritis to the presence of IL-17A$^+$ cells in the kidneys (5). Since we found that T cells in the secondary lymphoid organs of lupus-prone mice express IL-17A at high levels, we evaluated whether similar T cell populations infiltrate the kidneys in these mice. Fig. 5 shows immunohistochemical staining of kidneys from control and lupus-prone MRL/*lpr* mice with active nephritis (5 mo old, protein in the urine >2000 mg/dl, RBC >2000 cells/dl urine, white blood cells >500 cells/dl urine). As can be readily seen, the kidneys contained a significant number of CD3$^+$IL-17A$^+$ cells in the tubulointerstitial area; we did not observe such cells in the glomeruli. In addition, we did not find such an infiltrate in the kidneys of control MRL/MPJ mice. Finally, CD3$^+$IL-17A$^+$ cells could be detected, albeit at smaller numbers, in the kidneys of 2-mo-old MRL/*lpr* mice that did not show evidence of active nephritis (data not shown). Similar findings were also observed in B6/*lpr* lupus-prone animals that suffer from a less severe form of nephritis (data not shown).

IL-23-treated lymphocytes from lupus-prone mice induce nephritis in Rag-1$^{-/-}$ mice

Our data showed that IL-17A$^+$ cells are present in both lymphoid organs and kidneys of lupus-prone mice with active nephritis. Our in vitro experiments established that IL-23 expands DNT, which is the main population of IL-17A$^+$-expressing T cells in lupus-prone mice. To determine the role of IL-17A$^+$ cells in inducing nephritis in lupus-prone mice, we conducted lymphocyte transfer experiments as follows: cells were harvested from the lymph nodes of lupus-prone B6/*lpr* and control B6 mice and activated them in vitro using an anti-CD3 Ab with or without IL23 for 48 h. At the end of the culture, 5 million cells were injected i.p. in mice that lack both B and T cells (Rag-1$^{-/-}$ mice). Before injecting the lymph node extracts in the recipient mice, we evaluated the expression of IL-17A$^+$ in this cell population. As shown in Fig. 6*A*, B6/*lpr*-derived cells had significantly more IL-17A$^+$ cells compared with B6-derived cells. Furthermore there was a 2-fold increase in the number of IL-17A$^+$ cells after treatment with IL-23 vs the non-IL-23-treated control group. In accordance with the above-mentioned experiments (see Fig. 1), we found that the majority of cells producing IL-17A$^+$ in these lymph node extracts are DNT cells (CD4$^+$IL-17A$^+$ cells from lymph node extracts of B6/*lpr* mice: 30.3 ± 1.05% of total cell population vs CD4$^-$CD8$^-$IL-17A$^+$ cells: 67.4 ± 1.34% of total cell population, *n* = 4 animals). IL-23 treatment further increased the percentage of DNT cells in the IL-17A$^+$ cell population (CD4$^+$IL-17A$^+$ cells from lymph node extracts of B6/*lpr* mice treated with IL-23: 19.6 ± 2.11% of total cell population vs CD4$^-$CD8$^-$IL-17A$^+$ cells: 85.3 ± 0.83% of total cell population, *n* = 4 animals). Using CFSE staining, we evaluated the effect of IL-23 on proliferation of DNT cells. We found that IL-23 treatment increases the proliferation of DNT cells that are stimulated with anti-CD3 and anti-CD28 Abs for 4 days by 45% (dividing DNT cells stimulated with anti-CD3/anti-CD28 Abs for 4 days without IL-23: 34.4 ± 4.57% vs DNT cells stimulated with anti-CD3/anti-CD28 Abs for 4 days plus IL-23: 49.9 ± 5.16%). This finding suggests a "trophic" effect of IL-23 on DNT cells. Of note, <1% of the DNT cells were TCR γδ (as assessed by staining with anti-TCRγ Ab) and their percentage did not change with IL-23 treatment (data not shown).

We also evaluated the effect of IL-23 treatment on CD19$^+$ B cells. As shown in Fig. 6*B*, treatment with IL-23 did not significantly change the percentage of B cells in lymph node extracts and therefore the absolute number of B cells injected in the recipient mice. Of note, B6/*lpr* mouse-derived lymph node extracts had ~2.5 times more B cells than control B6-derived lymph node extracts (percentage of B cells from B6/lpr-derived lymph node cells vs B6: 12.98% ± 1.69 vs 4.85 ± 0.79%, *p* = 0.022) (data not shown).

The Rag-1$^{-/-}$ mice that were transplanted with lymphocytes from B6 and B6/*lpr* mice were sacrificed 4 wk after transfer. First, we evaluated whether lymphocytes were engrafted in the

secondary lymphoid organs. In Fig. 7, we show that CD3$^+$ cells were found in Rag-1$^{-/-}$ spleens after the transplant. In addition (Fig. 7, *fourth middle panel*), mice that received B6/*lpr*-derived lymphocytes pretreated with IL-23 had CD3$^+$IL-17A$^+$ cells in their spleens. Very few CD3$^+$IL-17A$^+$ cells were seen in mice transplanted with non-IL-23-treated B6/*lpr*-derived lymphocytes. Finally, no IL-17A$^+$ cells were seen in the spleens of Rag-1$^{-/-}$ mice transplanted with control B6-derived lymphocytes. This is in keeping with our observation that B6 and B6/*lpr* mice have very few resident IL-17A$^+$ cells in their lymph nodes (0.32% vs 0.38%; see above).

Subsequently, we evaluated whether CD3$^+$ and in particular IL-17A$^+$ cells could be found in the kidneys of the transplanted mice. Indeed, we found, similarly to the spleen, that only mice that received IL-23-treated B6/*lpr*-derived cells had IL-17A$^+$ cells in their kidneys (Fig. 8*A*). To further assess the presence of IL-17A$^+$ cells in the cell infiltrate in kidneys of recipient mice, we extracted kidney cells from Rag-1$^{-/-}$ mice that were transplanted with B6-and B6/*lpr*-derived cells. These kidney cells were analyzed using flow cytometry. As shown in Fig. 8*B* and *C*, flow cytometry confirmed that treatment of B6/*lpr* lymphocytes with IL-23 before their transfer in the recipient mice led to a 4-fold increase in IL-17A$^+$ cells in the kidneys of recipient mice (percentage of IL- 17A$^+$ cells in B6/*lpr*-derived IL-23-treated lymphocytes vs IL-17A$^+$ cells in B6/*lpr*-derived non-IL-23-treated lymphocytes: 0.049 ± 0.006 vs 0.014 ± 0.0007 $p < 0.0001$; $n = 4$). As expected, mice that received B6-derived lymphocytes did not have IL-17A$^+$ cells in their kidneys. Importantly, IL-17A$^+$ cells in the kidneys of recipient mice were mainly CD4$^-$CD8$^-$ cells. Since these cells were treated with IL-23 before the transfer, this finding was in keeping with our in vitro experiments showing a trophic effect of IL-23 on CD4$^-$CD8$^-$ cells.

To address whether IL-17A$^+$ infiltration of kidneys in recipient Rag-1$^{-/-}$ mice leads to overt nephritis, we evaluated the urine of the recipient mice for the presence of inflammatory cells (white blood cells) and protein. As shown in Table I, transfer of IL-23-treated lymphocytes in Rag-1$^{-/-}$ mice led to significant above the baseline proteinuria and appearance of white blood cells in the urine. The pyuria developed as early as 3 wk after transplant and disappeared soon afterward (at 4 wk). The proteinuria appeared shortly after the pyuria (by 4 wk), persisted for 4 wk, and gradually disappeared at 12 wk after transplant. Mice that were transplanted with B6-derived lymphocytes and B6/*lpr* lymphocytes that were not treated with IL-23 did not show evidence of significant proteinuria or pyuria.

Ig and C3d deposition is increased in the kidneys of Rag-1$^{-/-}$ mice transplanted with IL-23-treated lupus-prone mouse-derived lymphocytes

Lupus nephritis is characterized by the invariable deposition of Ig (IgG, IgM, IgA) and C3 in the glomeruli (4). We therefore evaluated the kidneys of the recipient mice for the presence of IgG, IgM, and C3d. In Fig. 9, we show that Rag-1$^{-/-}$ mice that received lupus-prone mouse-derived lymphocytes had deposition of Ig (both IgG and IgM) as well as C3d in their glomeruli. This was much more apparent in mice that received lymphocytes treated with IL-23 (Fig. 9, *row 4*). No Ig or complement deposition was seen in kidneys of Rag-1$^{-/-}$ mice that received control B6-derived lymphocytes (Fig. 9, *rows 1* and *2*).

Subsequently, we stained the kidneys of the recipient mice with H&E and PAS. Fig. 10*A* shows that Rag-1$^{-/-}$ mice that were transplanted with IL-23-treated lupus-prone mouse-derived lymphocytes had obliteration of the urine space of the glomerulus, mesangial expansion, and endocapillary cell proliferation. They also exhibited mild basement membrane thickening (PAS stain) and had rare interstitial cell infiltrates (photographs not shown). In addition, we measured the average glomerular area (according to the technique described in *Materials and Methods*). We found (Fig. 10*B*) that transfer of IL-23-treated lymphocytes derived from lupus-prone mice, but not control mice, led to ~25% increase in the average glomerular area. In

addition, we found that there was a nonstatistically significant increase in the average number of cells in the glomeruli of animals that were injected with B6/*lpr*-derived lymph node cells vs B6-derived lymph node cells; pre-treatment of the B6/*lpr* lymph node extracts with IL-23 resulted in even higher numbers of glomerular cells in the recipient mice (Table I).

Discussion

Several novel findings are presented herein. First, we found that T cells from lupus-prone animals express high levels of IL-17A and that IL-17A$^+$ cells can be identified in the kidneys of mice with active nephritis. These IL-17A$^+$ cells were overwhelmingly CD4$^-$CD8$^-$, a finding that is in keeping with the human data (5). We also showed that as the mice age and their disease worsens, their lymphocytes express progressively higher levels of IL-17A. These observations provide a link between IL-17A and immunopathology in murine lupus. This adds lupus to a list of experimental autoimmune diseases such as experimental encephalomyelitis (14,15) and experimental arthritis (16) where Th17 cells are present in areas of tissue damage.

IL-17A, which was found to be elevated in lupus-prone mice, belongs to the larger family that also includes IL-17B, C, D, E, and F. Of these cytokines, IL-17A and IL-17F are closely related and are produced primarily by T cells but also by other immune cells (reviewed in Ref. 11). They both bind the IL-17 receptors IL-17RA and IL-17RC that are widely distributed in hematopoietic, endothelial, and stromal cells and lead to the secretion of a variety of proinflammatory cytokines, chemokines, and acute phase reactants (reviewed in Ref. 17). One of the main effects of IL-17 is enhanced granulocyte trafficking to the sites of inflammation (18,19). In contrast to IL-17A, we did not find a difference in the levels of IL-17F between lupus-prone and control mice (data not shown). This is in keeping with the finding that IL-17F plays a role in host defense, but it is not essential for disease development in a either experimental encephalomyelitis or arthritis (14).

Second, while exploring the mechanisms via which IL-17A$^+$ cells were generated in lupus-prone mice, we observed that lymphocytes isolated from lupus-prone animals progressively express higher levels of IL-23 receptor mRNA as their disease becomes more severe. We then showed that by treating in vitro lymphocytes from lupus and non-lupus prone mice with IL-23, the levels of IL-23 receptor mRNA, IL-17A mRNA, and the number of IL-17A$^+$ cells increased. Even more importantly, IL-23 induced proliferation of DNT cells in vitro. These sets of experiments unraveled a novel function of IL-23 in lupus-prone mice where it may act as a "trophic/inducing" cytokine for a specific subset of T cells that do not bear the CD4 or CD8 molecules and produce IL-17 in lieu of the classic IL-2 and IFN-γ. This finding adds to the already established role of IL-23 as a differentiating factor for CD4$^+$ activated but not naive T cells.

Third, to establish whether IL-17A$^+$ cells play a role in the development of lupus nephritis, we took lymphocytes from mice with lupus and expanded them in vitro with anti-CD3 Ab and IL-23 before injecting them in *Rag-1$^{-/-}$* mice that lack both T and B cells. Only mice injected with IL-23-treated lymphocytes developed nephritis as manifested by active urine sediment. At the light microscopy level, the kidneys of the affected mice showed cellular aggregates, mesangial expansion, but most importantly, C3 and Ig deposition in the glomeruli. This finding suggests that rather than inducing a cellular response, IL-23 promoted an autoimmune humoral response with (auto)-antibodies depositing in the kidneys and activating the complement system resulting in nephritis. One possible mechanism that would explain this phenomenon is that IL-23-induced Th17 cells (primarily DNT as they were preferentially expanded by IL-23) provided excessive help to B cells, resulting in Ig deposition in the kidneys, rather than attracting leukocytes in the site of inflammation. Indeed, in the BXD2 autoimmune mouse model, IL-17 was shown to be important in the propagation of the autoimmune response by

promoting the formation of germinal centers (20) where B cells undergo further maturation via cognate interaction with T cells. It can be further speculated that the generation of Th17 resulted in a reciprocal decrease in the number of regulatory T cells, as the two phenotypes may be mutually exclusive on the cellular level (11,21). In addition, IL-12p40-deficient MRL/*lpr* mice that would therefore lack both IL-12 and IL-23 had a delayed onset of nephritis with a decreased number of B220^{+} DNT cells infiltrating their kidneys. Although there was amelioration of their disease and prolonged survival, these animals eventually developed severe nephritis and died (22). This article although supporting the role of IL-23 in lupus nephritis, it also points to the fact that other factors play a role in lupus nephritis; it does not though directly address the role of IL-17A^{+} cells in murine lupus.

Several questions remain to be addressed as to the precise role and the molecular pathways that are involved in the activation of Th17 cells in lupus. Although we showed that lymphocytes from lupus-prone mice produce significant amounts of IL-17A upon treatment with IL-23, the exact origin and role of IL-23 in the generation of Th17 cells and in particular CD3^{+}CD4^{−}CD8^{−}IL-17A^{+} cells are still unclear. It is possible that other cytokines such as IL-6 that are up-regulated in lupus may be indispensable or as important as IL-23 in the generation of Th17 cells. Our results show that IL-23-treated lupus-prone mouse lymphocytes promote a humoral rather than cellular immunologic response in recipient mice. The mechanisms via which this takes place as well as the specificity of the Ig deposited in the kidneys of these recipient mice will need to be further elucidated.

In conclusion, herein we showed that the IL-23/IL-17A pathway is activated in lupus-prone mice and is associated with increased Ig deposition and complement activation in the kidney.

Acknowledgments

References

1. Balow JE. Clinical presentation and monitoring of lupus nephritis. Lupus 2005;14:25–30. [PubMed: 15732284]

2. Dimitriou, SG.; Madaio, MP. Renal damage in systemic lupus erythematosus. In: Tsokos, GC.; Gordon, C.; Smolen, J., editors. Systemic Lupus Erythematosus: A Companion to Rheumatology. Philadelphia: Mosby; 2007. p. 287-292.

3. Houssiau FA, Ginzler EM. Current treatment of lupus nephritis. Lupus 2008;17:426–430. [PubMed: 18490421]

4. Illei, GG.; Balow, JE. Kidney involvement in systemic lupus erythematosus. In: Tsokos, GC.; Gordon, C.; Smolen, J., editors. Systemic Lupus Erythematosus: A Companion to Rheumatology. Philadelphia: Mosby; 2007. p. 336-350.

5. Crispin JC, Oukka M, Bayliss G, Cohen RA, Van Beek CA, Stillman IE, Kyttaris VC, Juang YT, Tsokos GC. Expanded double negative T cells in patients with systemic lupus erythematosus produce IL-17 and infiltrate the kidneys. J. Immunol 2008;181:8761–8766. [PubMed: 19050297]

6. Inghirami G, Simon J, Balow JE, Tsokos GC. Activated T lymphocytes in the peripheral blood of patients with systemic lupus erythematosus induce B cells to produce immunoglobulin. Clin. Exp. Rheumatol 1988;6:269–276. [PubMed: 3263240]

7. Rajagopalan S, Zordan T, Tsokos GC, Datta SK. Pathogenic anti-DNA autoantibody-inducing T helper cell lines from patients with active lupus nephritis: isolation of CD4^{−}8^{−} T helper cell lines that express the γδ -cell antigen receptor. Proc. Natl. Acad. Sci. USA 1990;87:7020–7024. [PubMed: 2144899]

8. Shivakumar S, Tsokos GC, Datta SK. T cell receptor α/β expressing double-negative (CD4^{−}/CD8^{−}) and CD4^{+} T helper cells in humans augment the production of pathogenic anti-DNA autoantibodies associated with lupus nephritis. J. Immunol 1989;143:103–112. [PubMed: 2525144]

9. Wong CK, Ho CY, Li EK, Lam CW. Elevation of proinflammatory cytokine (IL-18, IL-17, IL-12) and Th2 cytokine (IL-4) concentrations in patients with systemic lupus erythematosus. Lupus 2000;9:589–593. [PubMed: 11035433]

10. Wong CK, Lit LC, Tam LS, Li EK, Wong PT, Lam CW. Hyperproduction of IL-23 and IL-17 in patients with systemic lupus erythematosus: implications for Th17-mediated inflammation in auto-immunity. Clin. Immunol 2008;127:385–393. [PubMed: 18373953]

11. Korn T, Bettelli E, Oukka M, Kuchroo VK. IL-17 and Th17 Cells. Annu. Rev. Immunol 2009;27:485–517. [PubMed: 19132915]

12. Cohen PL, Eisenberg RA. *lpr* and *gld*: single gene models of systemic autoimmunity and lymphoproliferative disease. Annu. Rev. Immunol 1991;9:243–269. [PubMed: 1910678]

13. Igarashi S, Takiguchi M, Kariyone A, Kano K. Phenotypic and functional analyses on T-cell subsets in lymph nodes of MRL/Mp-*lpr*/*lpr* mice. Int. Arch. Allergy Appl. Immunol 1988;86:249–255. [PubMed: 3136087]

14. Ishigame H, Kakuta S, Nagai T, Kadoki M, Nambu A, Komiyama Y, Fujikado N, Tanahashi Y, Akitsu A, Kotaki H, et al. Differential roles of interleukin-17A and -17F in host defense against mucoepithelial bacterial infection and allergic responses. Immunity 2009;30:108–119. [PubMed: 19144317]

15. Komiyama Y, Nakae S, Matsuki T, Nambu A, Ishigame H, Kakuta S, Sudo K, Iwakura Y. IL-17 plays an important role in the development of experimental autoimmune encephalomyelitis. J. Immunol 2006;177:566–573. [PubMed: 16785554]

16. Nakae S, Nambu A, Sudo K, Iwakura Y. Suppression of immune induction of collagen-induced arthritis in IL-17-deficient mice. J. Immunol 2003;171:6173–6177. [PubMed: 14634133]

17. Gaffen SL. An overview of IL-17 function and signaling. Cytokine 2008;43:402–407. [PubMed: 18701318]

18. Yu JJ, Ruddy MJ, Wong GC, Sfintescu C, Baker PJ, Smith JB, Evans RT, Gaffen SL. An essential role for IL-17 in preventing pathogen-initiated bone destruction: recruitment of neutrophils to inflamed bone requires IL-17 receptor- dependent signals. Blood 2007;109:3794–3802. [PubMed: 17202320]

19. Kelly MN, Kolls JK, Happel K, Schwartzman JD, Schwarzenberger P, Combe C, Moretto M, Khan IA. Interleukin-17/interleukin-17 receptor-mediated signaling is important for generation of an optimal polymorphonuclear response against *Toxoplasma gondii* infection. Infect. Immun 2005;73:617–621. [PubMed: 15618203]

20. Hsu HC, Yang P, Wang J, Wu Q, Myers R, Chen J, Yi J, Guentert T, Tousson A, Stanus AL, et al. Interleukin 17-producing T helper cells and interleukin 17 orchestrate autoreactive germinal center development in autoimmune BXD2 mice. Nat. Immunol 2008;9:166–175. [PubMed: 18157131]

21. Yang XO, Nurieva R, Martinez GJ, Kang HS, Chung Y, Pappu BP, Shah B, Chang SH, Schluns KS, Watowich SS, et al. Molecular antagonism and plasticity of regulatory and inflammatory T cell programs. Immunity 2008;29:44–56. [PubMed: 18585065]

22. Kikawada ED, Lenda M, Kelley VR. IL-12 deficiency in MRLFas^{lpr} mice delays nephritis and intrarenal IFN-γ expression, and diminishes systemic pathology. J. Immunol 2003;170:3915–3925. [PubMed: 12646661]
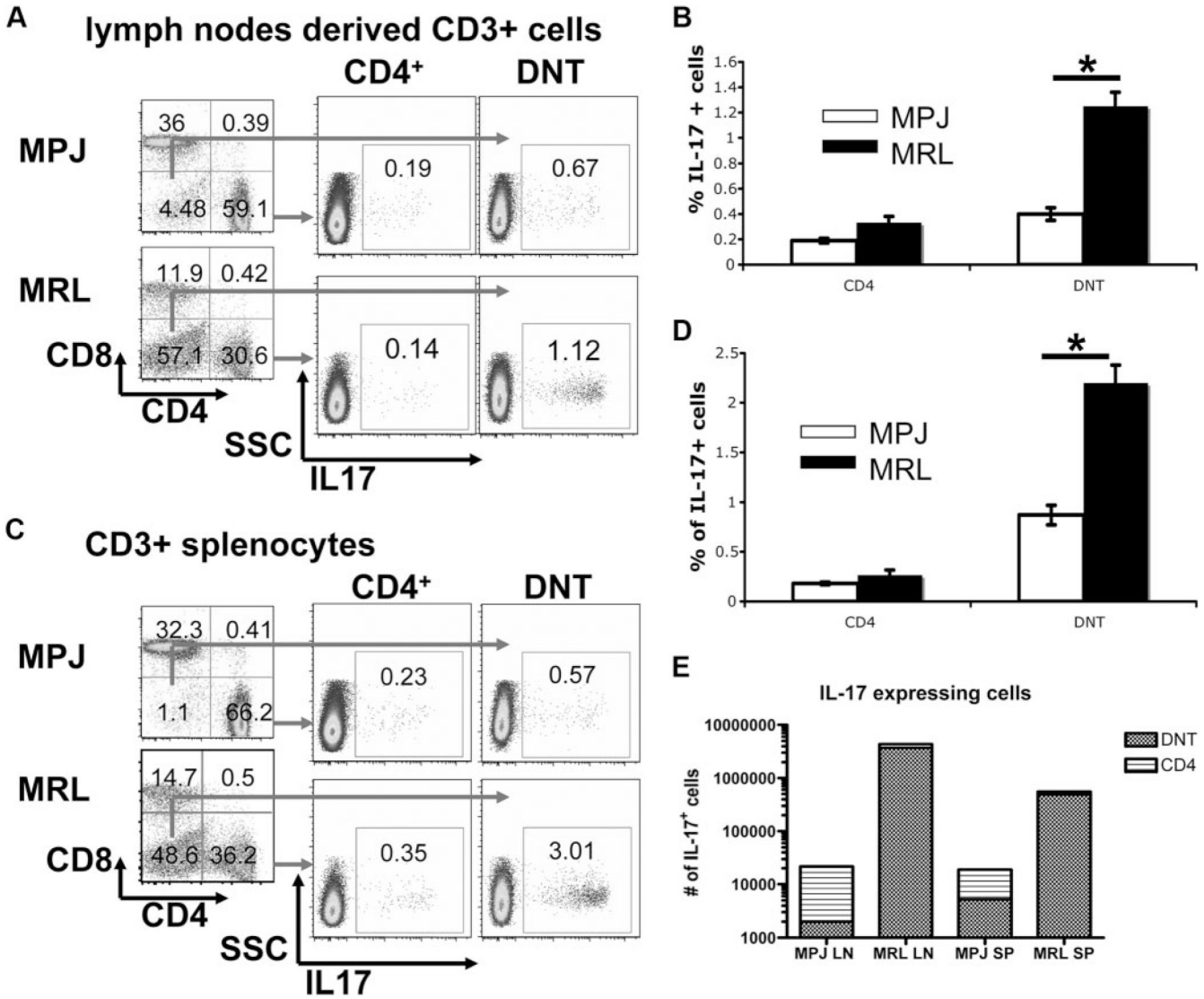
FIGURE 1.
CD3^{+}CD4^{−}CD8^{−} T cells from lupus-prone MRL/*lpr* mice express IL-17A at a higher level than CD3^{+}CD4^{+} T cells from both lupus-prone and control mice. Lymph nodes (LN) and spleens were harvested from lupus-prone MRL/*lpr* and control MRL/MPJ mice. The cells were isolated from the tissue as described in *Materials and Methods* and stained with anti-CD3, anti-CD4, and anti-CD8 Abs and with anti-IL-17A Ab (by intracellular staining) and analyzed by FACS. *A*, FACS analysis showing IL-17A expression in CD3^{+} lymph node-derived cells from both control (MPJ) and lupus-prone (MRL) mice. One representative experiment of four experiments is shown. *B*, Cumulative results showing IL-17A expression in lymph node-derived cells (*n* = 8 MPJ, *n* = 9 MRL mice, 4 mo old). *C*, FACS analysis showing IL-17A expression in CD3^{+} splenocytes from both control (MPJ) and lupus-prone (MRL) mice. One representative experiment of four experiments is shown. *D*, Cumulative results showing IL-17A expression in splenocytes (*n* = 8 MPJ, *n* = 9 MRL mice, 4 mo old). *E*, The total number of CD3^{+}CD4^{+} (CD4^{+}) and CD3^{+}CD4^{−}CD8^{−} (DNT) cells isolated from the lymph nodes (*first two bars*) and the spleens (*last two bars*) were measured. The total number of CD4^{+} and DNT was multiplied by the percentage of IL-17A-expressing cells for each group as measured by

FACS. We show a bar graph comparing the total number of cells (CD4$^+$ and DNT) that express IL-17A in both control and lupus-prone mice. *, $p < 0.0001$. SSC, Side scatter.

A

IL-23 receptor expression in lymph nodes

B

IL-17 expression in lymph nodes
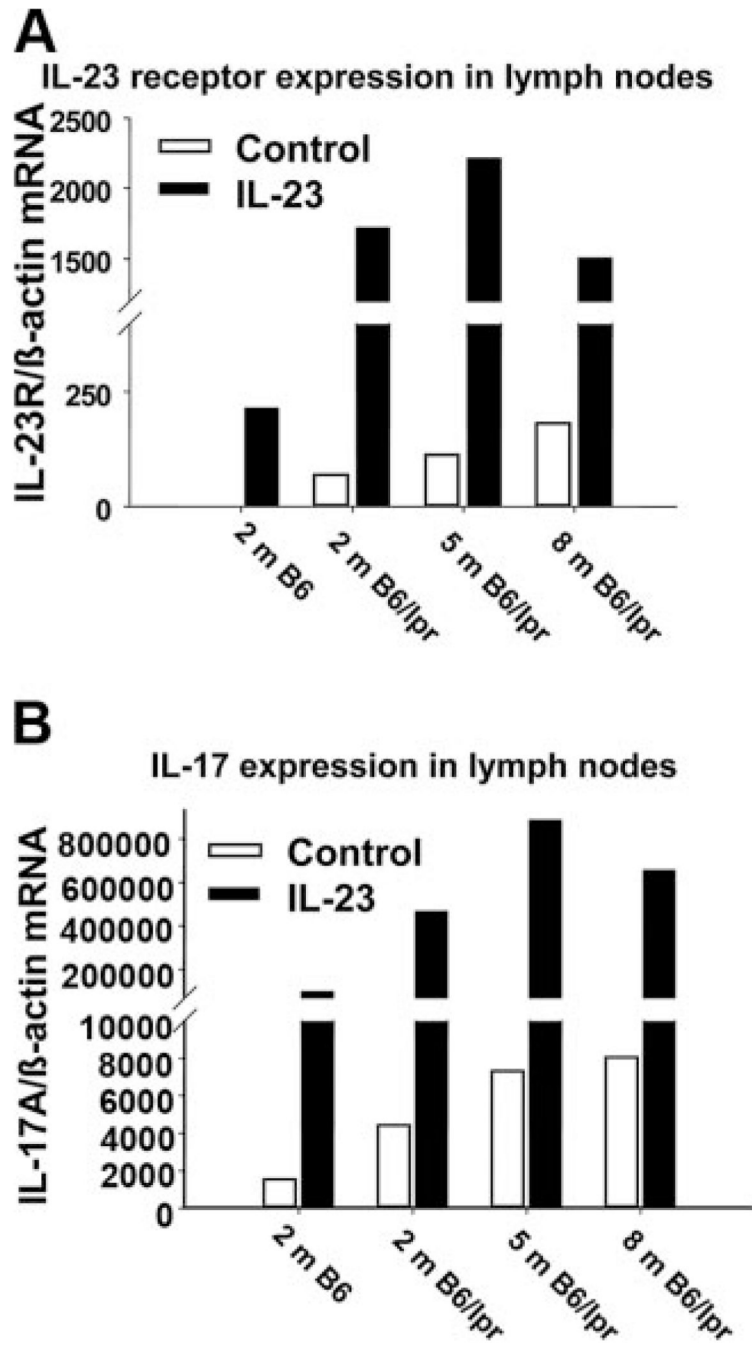
FIGURE 2.
IL-23 receptor and IL-17A expression is up-regulated in T cells from lupus-prone mice and correlated with disease progress. Cells were extracted from the lymph nodes of 2-mo-old B6 mice, predisease 2-mo-old lupus-prone B6/*lpr*, established disease 5- mo-old B6/*lpr*, and severely diseased 8-mo-old B6/*lpr* mice (four mice used in each group). The cells were incubated in DMEM with plate-bound anti-CD3 Ab in the presence (■) or absence of IL-23 (□) for 6 days. Total mRNA was extracted, reverse transcribed, and analyzed by TaqMan PCR with specific primers for the IL-23 receptor (IL-23R) and IL-17A. The expression of IL-23R as a ratio of IL-23R mRNA:β-actin mRNA is shown in *A*. The expression of IL-17A as a ratio

of IL-17A mRNA:β-actin mRNA is shown in *B*. The data represent one of three independent experiments.
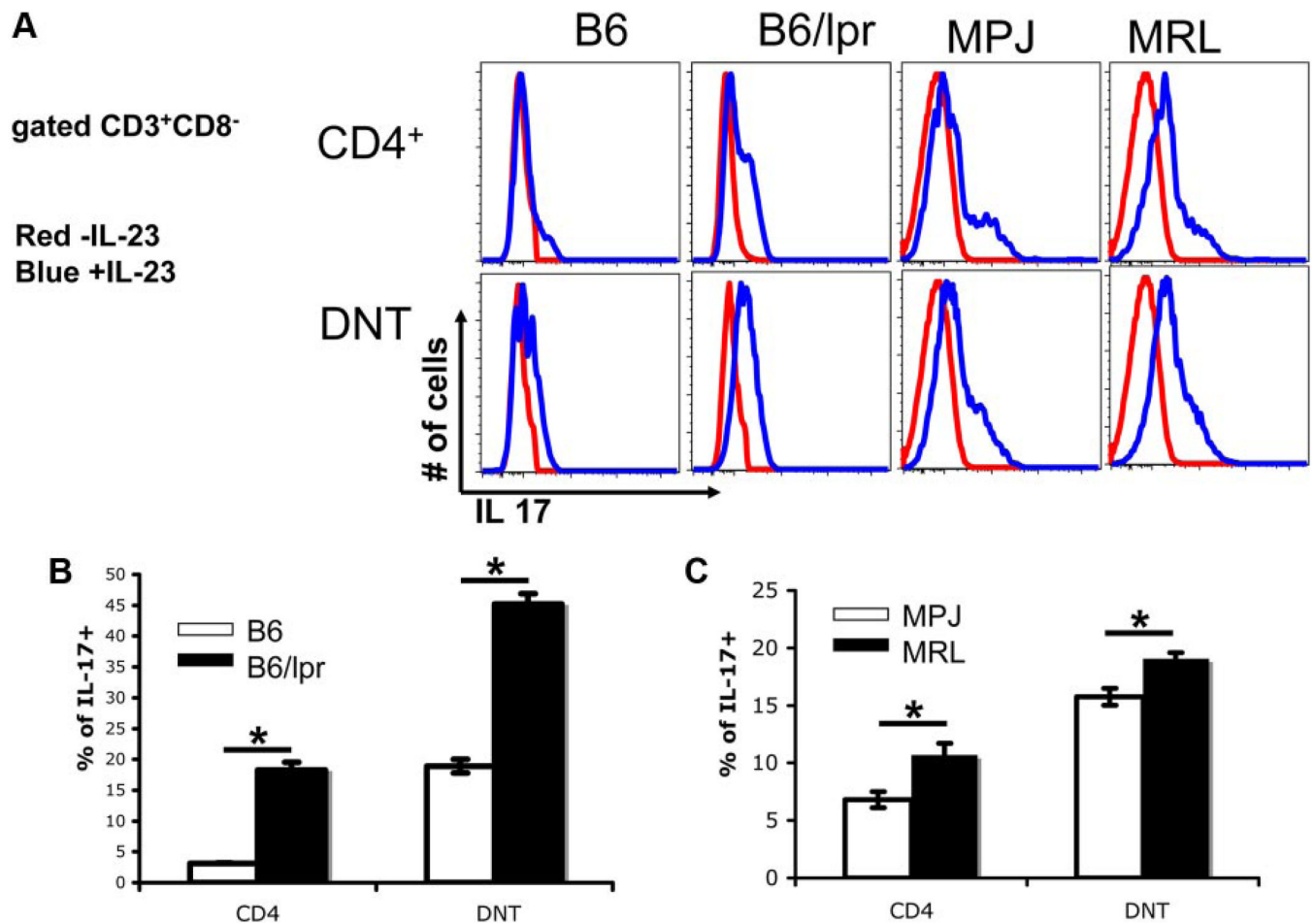
FIGURE 3.
IL-23 induces IL-17A production in CD4$^+$ and particularly in CD4$^-$CD8$^-$ T cells. Cells were extracted from the lymph nodes of 5-mo-old B6, B6/*lpr*, 4-mo-old MRL/MPJ, and MRL/*lpr* mice. The cells were incubated in DMEM with plate-bound anti-CD3 Ab in the presence or absence of IL-23 for 6 days. IL-17A$^+$ T cells were measured using intracellular staining according to methods described in *Materials and Methods*. *A*, Histograms of IL-17A expression in IL-23-treated (blue line) vs control-treated (red line) T cells are depicted. Specifically, histograms for B6 (*first column*), B6/*lpr* (*second column*), MRL/MPJ (*third column*), MRL/*lpr* (*fourth column*) CD4$^+$ (*first row*), and CD4$^-$CD8$^-$ (*second row*) are depicted. *B*, Cumulative results from IL-23-treated T cells from eight mice for the B6 and B6/*lpr* groups. *C*, Cumulative results from IL-23-treated T cells from seven mice for the MRL/MPJ and MRL/*lpr* groups are shown. *, $p < 0.0001$.
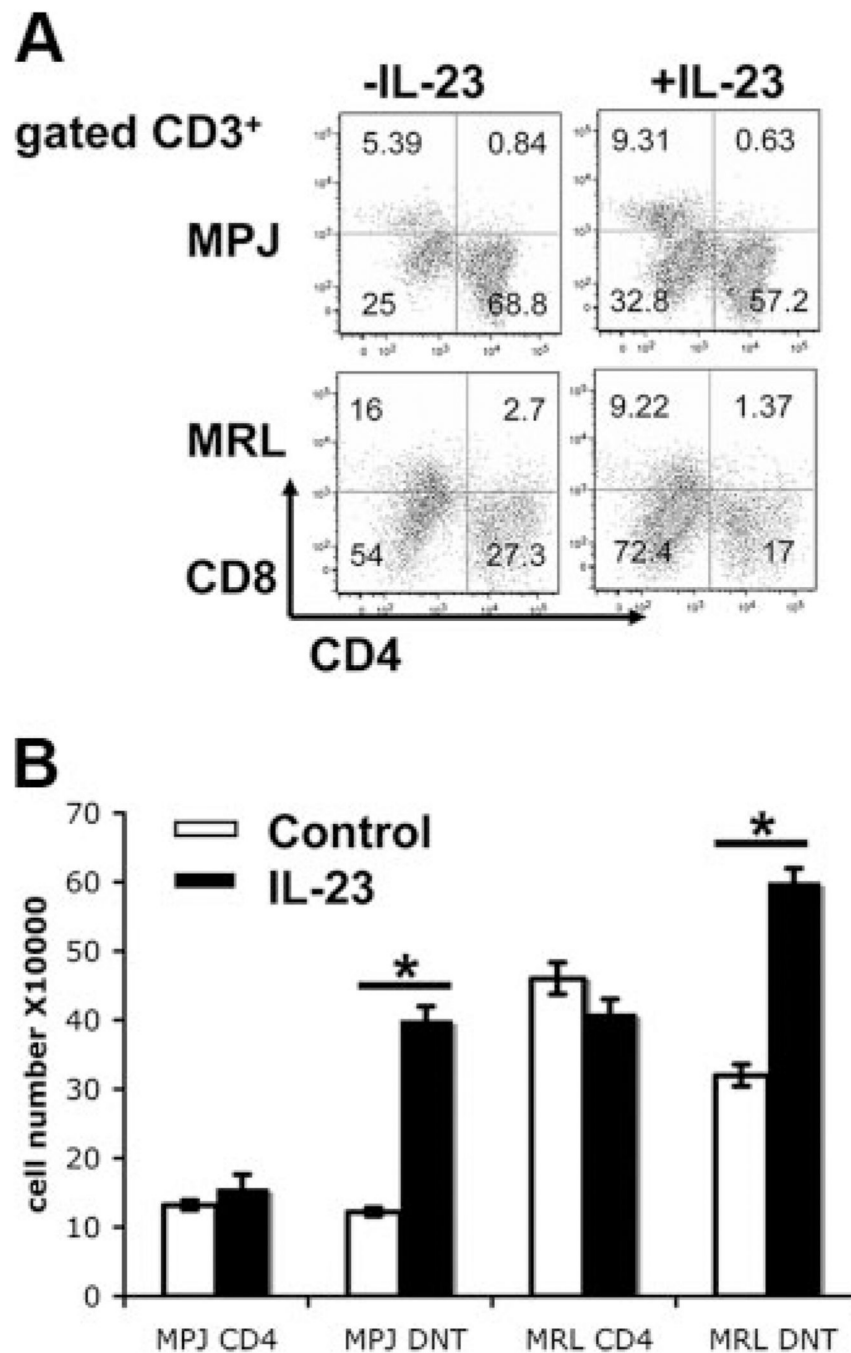
FIGURE 4.
IL-23 stimulation expands the CD4⁻CD8⁻ T cells derived from both control MRL/MPJ and
lupus-prone MRL/*lpr* mice. *A*, Cells were extracted from the lymph nodes of 4-mo-old MRL/
lpr and MRL/MPJ mice. The cells were incubated in DMEM with plate-bound anti-CD3 Ab
in the presence or absence of IL-23 for 6 days. Cells were stained with anti-CD3, anti-CD4,
anti-CD8 fluorescent Abs. We show FACS analysis of the CD3⁺ cells derived from MRL/
lpr and MRL/MPJ mice and treated with or without IL-23. One of three independent
experiments is shown. *B*, Cells were extracted from the lymph nodes of 4-mo-old MRL/*lpr*
and MRL/MPJ mice and sorted into CD3⁺CD4⁺ and CD3⁺CD4⁻CD8⁻ (DNT) cells. The cells
were incubated (at a concentration of 2×10^5 cells/well) in DMEM with plate-bound anti-CD3

and anti-CD28 Abs in the presence or absence of IL-23 for 6 days. At the end of the incubation, the cells in each well were counted. The total number of cells from each group is shown in the graph (mean ± SD of three independent measurements, one of three independent experiments). *, $p < 0.001$).
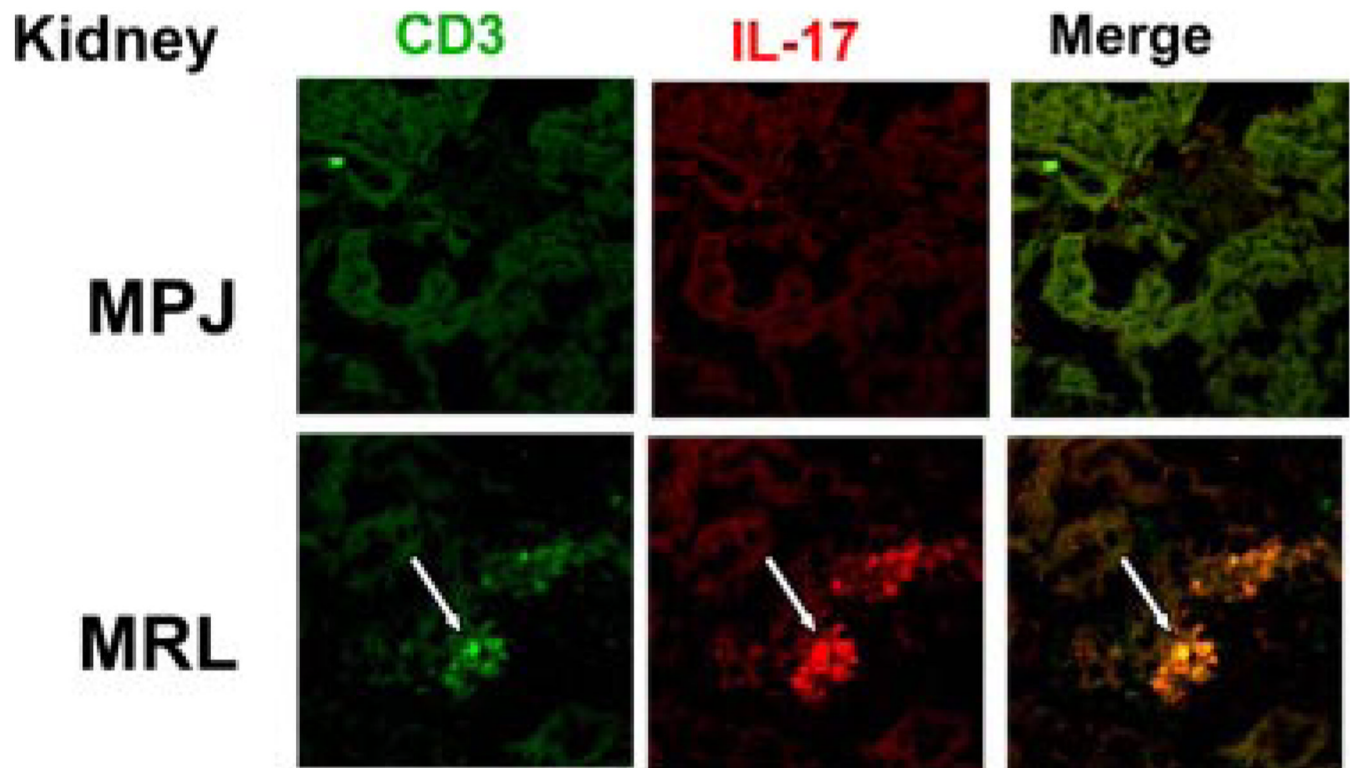
FIGURE 5.
IL-17A- expressing T cells infiltrate the kidneys of lupus-prone mice. Frozen kidney sections from both 5-mo-old MRL/MPJ and MRL/*lpr* mice were stained with anti-CD3-FITC and anti-IL-17 Abs, followed by goat anti-rat IgG Texas Red fluorescent secondary Ab. The slides were imaged using a confocal microscope (one of four independent experiments). White arrows point to individual cells.
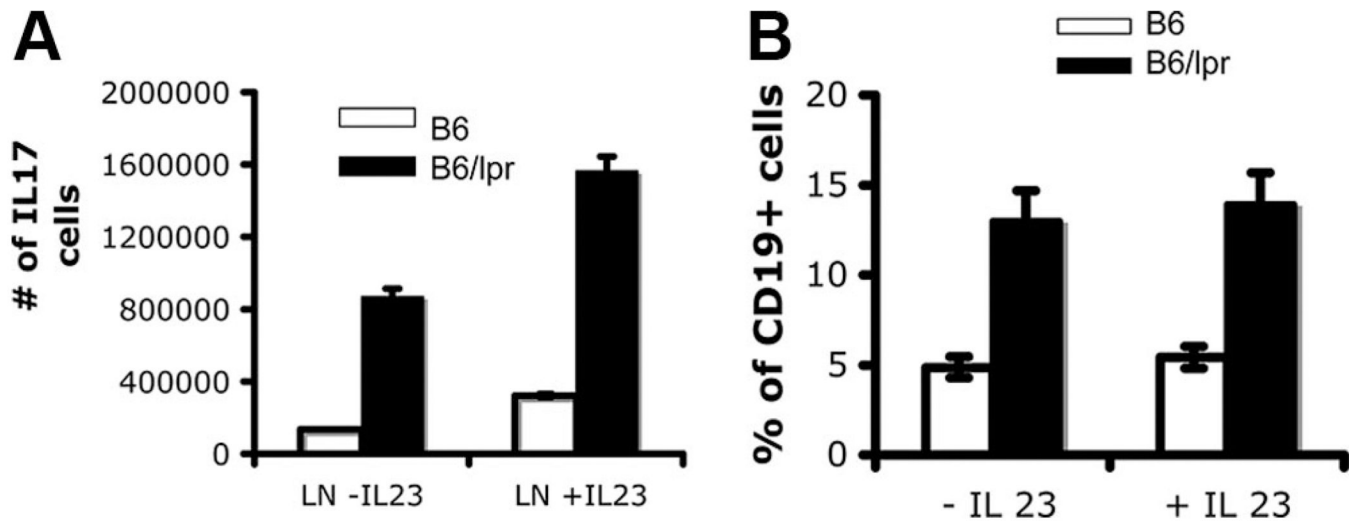
FIGURE 6.
IL-23 treatment leads to an increase in the number of IL- 17A[+] lymphocytes and does not affect the percentage of B cells. Lymphocytes from 5- mo-old control B6 and lupus-prone B6/lpr mice were extracted (three mice in each group) and stimulated with anti-CD3 (2 µg/ml) with or without IL-23 (20 ng/ml) for 48 h. These cells were thereafter injected i.p. in Rag-1^{−/−} mice (5 million in each mouse). *A*, The number of IL-17A-expressing T cells that were injected into each Rag1^{−/−} mouse was determined by intracellular cytokine staining, followed by FACS analysis. We show the number of IL17A^{+} T cells that were transferred from all four different groups into the Rag-1^{−/−} mice. *B*, The percentage of CD19^{+} cells in the lymph node extracts treated with or without IL-23 were determined using FACS analysis (four animals in each group).

RAG-1⁻/⁻ spleen
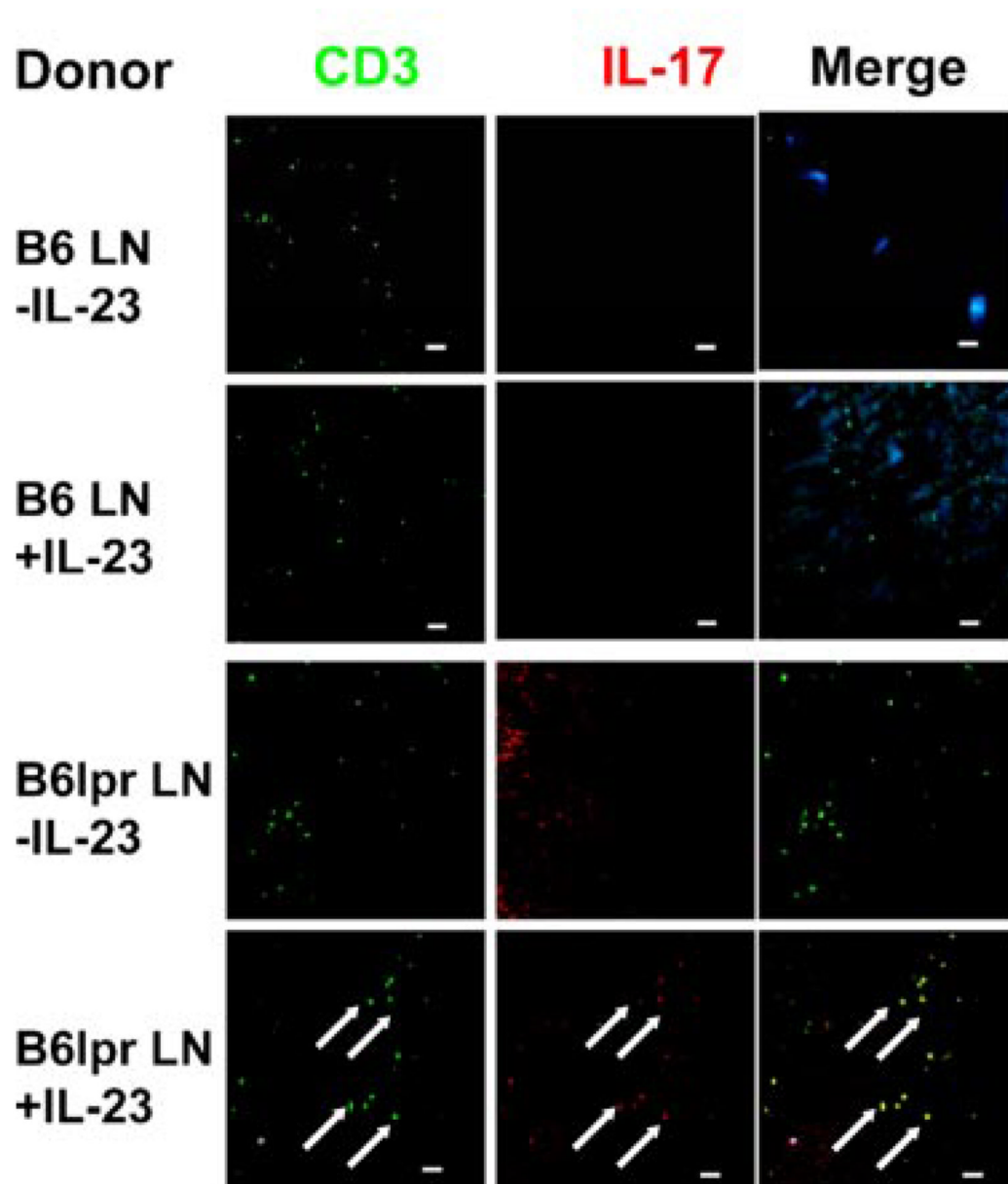
FIGURE 7.
IL-17A$^+$CD3$^+$ cells are found in the spleen of Rag-1$^{-/-}$ mice that were injected with IL-23-treated B6/*lpr*-derived lymphocytes. Rag-1$^{-/-}$ mice that were injected with lymphocytes derived from control B6 and B6/*lpr* mice were sacrificed 4 wk after transfer. Spleen sections were prepared according to the data in *Materials and Methods*. The sections were stained with CD3-FITC Ab and anti-IL-17A Ab according to the methods described in *Materials and Methods* and imaged using a confocal microscope. Staining of splenic sections of Rag-1$^{-/-}$ mice that were injected with B6-derived lymphocytes (*first row*), B6-derived lymphocytes treated with IL-23 (*second row*), B6/*lpr*-derived lymphocytes (*third row*), and B6/*lpr*-derived

lymphocytes treated with IL-23 (*fourth row*). Bar, 50 µm. White arrows point to individual cells. LN, Lymph node.
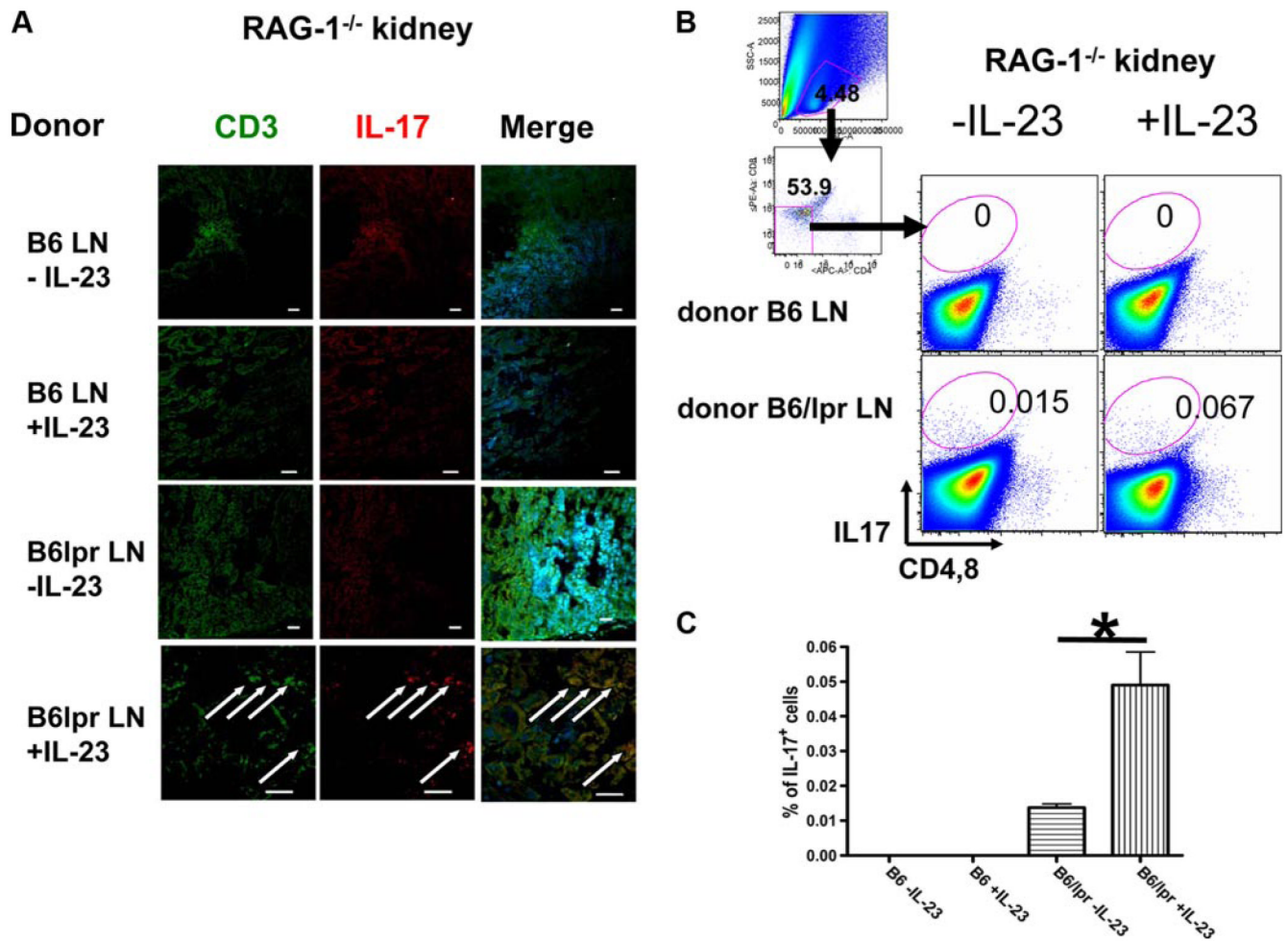
FIGURE 8.
IL-17A$^+$CD3$^+$ cells are found in kidneys of Rag-1$^{-/-}$ mice that were injected with IL-23-treated B6/*lpr*-derived lymphocytes. Rag-1$^{-/-}$ mice that were injected with lymphocytes derived from control B6 and B6/*lpr*mice were sacrificed 4 wk after transfer. Kidney sections were prepared according to data described in *Materials and Methods*. The sections were stained with CD3-FITC Ab and anti-IL-17A Ab according to the data in *Materials and Methods*and imaged using a confocal microscope. *A*, Staining of kidney sections of Rag-1$^{-/-}$ mice that were injected with B6-derived lymphocytes (*first row*), B6-derived lymphocytes treated with IL-23 (*second row*), B6/*lpr*-derived lymphocytes (*third row*), and B6/*lpr*-derived lymphocytes treated with IL-23 (*fourth row*). One representative experiment of 5 (for the B6 groups) and 1of 12 (for the B6/*lpr*groups) are shown. Bar, 50 µm. *B*, IL-17A-expressing cells infiltrate the kidneys of Rag-1$^{-/-}$ mice that are injected with lymphocytes derived from lupus-prone mice. Rag-1$^{-/-}$ mice that were injected with lymphocytes derived from control B6 and B6/*lpr* mice were sacrificed 4 wk after transfer. The kidneys were treated with collagenase for 30 min before cell extraction. IL-17A-expressing cells were determined by intracellular cytokine staining, followed by FACS analysis (gate on lymphoid population). A representative FACS analysis is shown. *C*, Cumulative results from recipient mice that were injected with lymphocytes from control B6 and B6/*lpr* lymphocytes treated with or without IL-23 (*, $p < 0.001$). White arrows point to individual cells. LN, Lymph node.
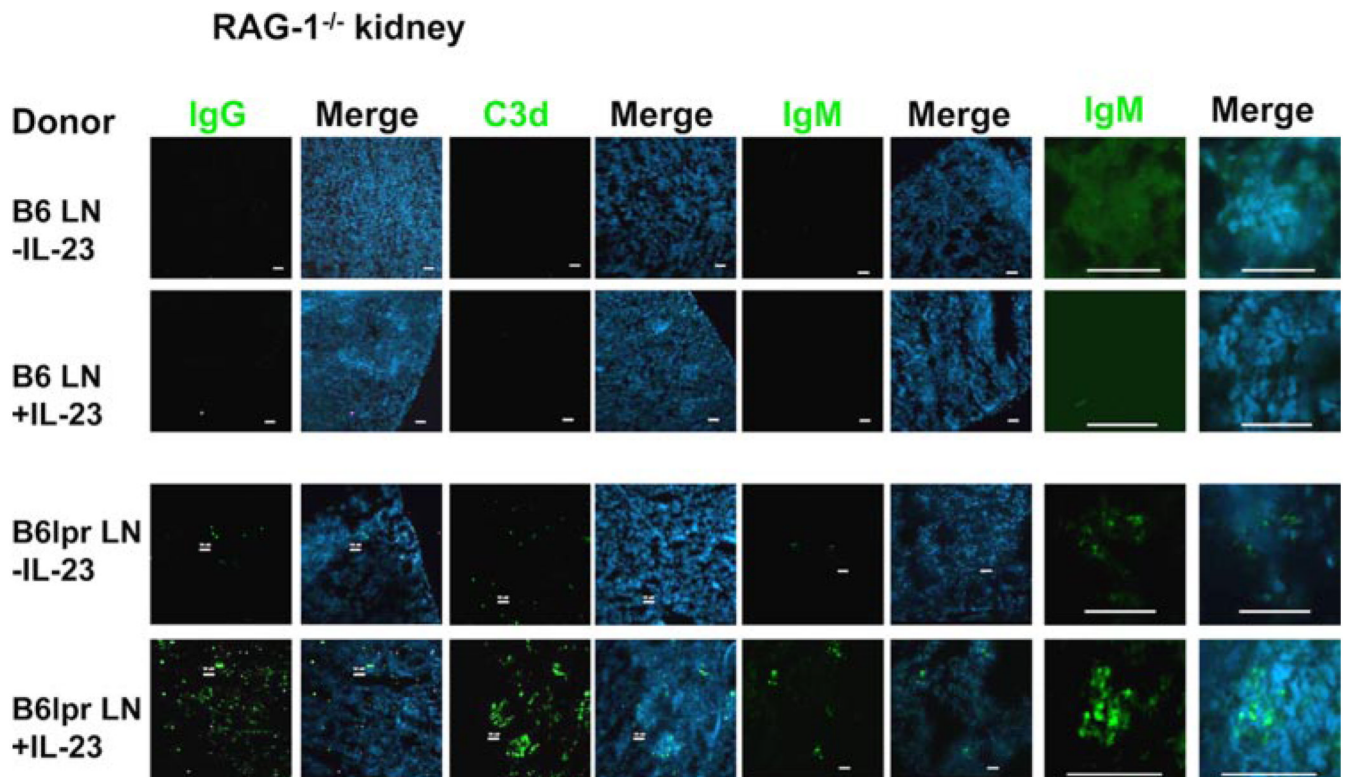
FIGURE 9.
Rag-1$^{-/-}$ mice injected with IL-23-treated B6/*lpr*-derived lymphocytes show significant IgG, IgM, and C3 deposition in the kidneys. Rag-1$^{-/-}$ mice that were injected with lymphocytes derived from control B6 and B6/*lpr* mice were sacrificed 4 wk after transfer. Frozen kidney sections were prepared according to the data in *Materials and Methods* and used for immunofluorescent studies. The sections were stained with IgG-Alexa Fluor 488, C3d-Alexa Fluor 488, IgM-Alexa Fluor 488, and DAPI. We show staining of kidney sections of Rag-1$^{-/-}$ mice that were injected with B6-derived lymphocytes (*first row*), B6-derived lymphocytes treated with IL-23 (*second row*), B6/*lpr*-derived lymphocytes (*third row*), and B6/*lpr*-derived lymphocytes treated with IL-23 (*fourth row*). The merge columns depict merging of the respective Ab staining with DAPI staining (one representative experiment of 5 (for the B6 groups) and 1 of 12 (for the B6/*lpr* groups) are shown). Bar, 50 µm. LN, Lymph node.
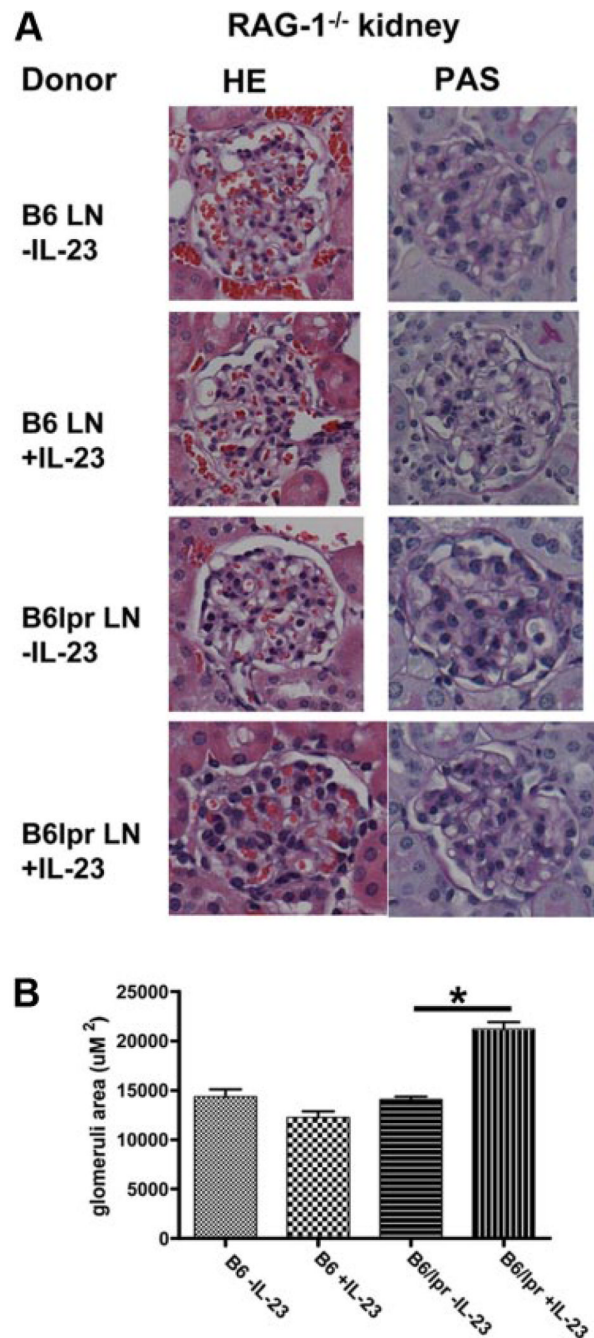
FIGURE 10.
Rag-1$^{-/-}$ mice injected with IL-23-treated B6/*lpr*-derived lymphocytes have enlarged glomeruli in their kidneys. Rag-1$^{-/-}$ mice that were injected with lymphocytes derived from control B6 and B6/*lpr* mice were sacrificed 4 wk after transfer. Kidney sections were prepared according to the data in *Materials and Methods* and stained with H&E and PAS according to methods described in *Materials and Methods*. *A*, We show the H&E (*first column*) and PAS (*second column*) staining of kidney sections of Rag-1$^{-/-}$ mice that were injected with B6-derived lymphocytes (*first row*), B6-derived lymphocytes treated with IL-23 (*second row*), B6/*lpr*derived lymphocytes (*third row*), and B6/*lpr*-derived lymphocytes treated with IL-23 (*fourth row*); original magnification, ×400 for both H&E and PAS); one representative

experiment of 5 (for the B6 groups) and one of 12 (for the B6/*lpr* groups) are shown. *B*, The glomerular area from the abovementioned sections was measured according to methods described in *Materials and Methods*. The mean ± SD of the area of 100 glomeruli (derived from 5 mice in the B6 groups and 12 mice in the B6/*lpr* groups) is plotted (*, $p < 0.0001$). LN, Lymph node.

Table I

Urine analysis and kidney pathology of Rag 1$^{-/-}$ recipient mice that were injected with lymph node extracts from control and lupus-prone mice

Donor mouse→	B6 (*n* = 5)	B6 (*n* = 5)	B6/*lpr* (*n* = 12)	B6/*lpr* (*n* = 12)
Cell treatment→	−	IL-23	−	IL-23
White blood cells in urine	0 cells/μl	0 cells/μl	0 cells/μl	5–15 cells/μl (3 wk after transfer), +++ (4 wk after transfer)
Proteinuria	+	+	+	
Glomeruli cell no.	34–46 cells	32–45 cells	46–57 cells	56–72 cells, mild
Interstitial inflammation^a	0%	0%	0%	100%^{b,c}

^{a}Interstitial inflammation is defined as the presence of lymphocyte aggregates in the interstitium of the kidney.

^{b}Lymphocyte aggregates present in 20% of the individual high-power (×40) fields.

^{c}Fisher's exact test two tailed, $p < 0.0001$ (B6/*lpr* treated with IL-23 vs B6/*lpr* not treated with IL-23); $p = 0.0002$ (B6/*lpr* treated with IL-23 vs B6 treated with IL-23); $p = 0.0002$ (B6/*lpr* treated with IL-23 vs B6 not treated with IL-23).